Numerical analysis and simulation of the dynamics of mountain glaciers

Guillaume Jouvet and Jacques Rappaz

Abstract In this paper, we analyse and approximate a nonlinear stationary Stokes problem that describes the motion of glacier ice. The existence and uniqueness of solution are proved and an *a priori* error estimate for the finite element approximation is found. In a second time, we combine the Stokes problem with a transport equation for the volume fraction of ice which describes the time evolution of a glacier. The accumulation due to snow precipitation and the melting are accounted in the source term of the transport equation. A decoupling algorithm allows the diffusion and the advection problems to be solved using a two-grids method. As an illustration, we simulate Aletschgletscher, Switzerland, over the 21st century by using realistic climatic conditions.

Introduction

Most of mountain glaciers of the world are currently shrinking and it is expected that this trend will continue as global warming progresses. However, the changes of glaciers do not only result from climatic conditions. Indeed, ice moves like a viscous fluid under gravitational forces such that steep bedrocks of mountain glaciers generate downhill ice flows. In the same time, accumulation of ice due to snow precipitation and melting continuously increase or decrease the glacier surface. To simulate and predict the future of glaciers, one needs to combine the equations of the fluid mechanic which describe the ice flows and a mass balance model that accounts for mass conservation and external exchanges of ice due to climate.

Guillaume Jouvet
Institut für Mathematik, Freie Universität Berlin, 14195 Berlin, Germany, e-mail: guillaume.jouvet@fu-berlin.de

Jacques Rappaz
Institut d'Analyse et Calcul Scientifique, EPFL, 1015 Lausanne, Switzerland, e-mail: jacques.rappaz@epfl.ch

The goal of this paper is to provide an overview of theoretical results, numerical techniques and applications of a glacier model. The model we consider in the article is fully three-dimensional, i.e. it does not include any simplification due to the small aspect ratio of glacier like most of existing models, see [10].

This paper is divided into two sections. Section 1 concerns the stationary non linear Stokes problem that describes the motion of ice. The model is described in Subsection 1.1, we prove the existence and the uniqueness of a solution in Subsection 1.2 and propose an approximation by finite elements in Subsection 1.3. In contrast, Section 2 combines the previous Stokes model with a transport equation to describe the time evolution of a real glacier. Subsections 2.1 and 2.2 are dedicated to the physical model and the numerical approximation, respectively. As an illustration, a simulation of Aletschgletscher is presented in Subsection 2.3.

1 Stationary problem

1.1 Model

Call $\Omega \in \mathbb{R}^3$ a finite volume of ice that is lying on a given topography, see Fig. 1. The boundary of Ω splits into the ice-air interface called Γ_N and the ice-bedrock interface. On this latter, ice might be stuck to the ground or slide. For this reason, we distinguish two cases and we call Γ_D the non-sliding and Γ_R the sliding parts of the ice-bedrock interface. Finally, we have $\partial\Omega = \Gamma_N \cup \Gamma_D \cup \Gamma_R$. In what follows, we assume Γ_N and Γ_R are $\mathscr{C}^1$ and $\Gamma_D \neq \emptyset$.

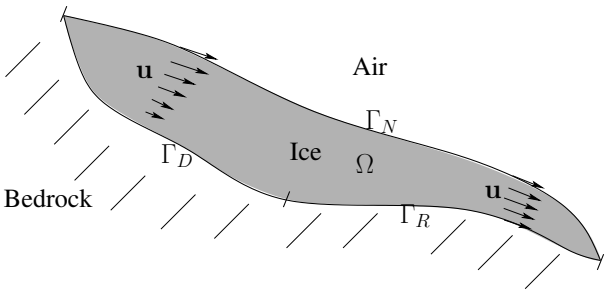

Fig. 1 Section of a three-dimensional domain of ice with notations.

Ice is commonly considered as an incompressible non-Newtonian fluid that follows the Glen's flow law [10]. In fact, ice is so viscous that acceleration effects can be neglected. More precisely, the velocity $\mathbf{u}$ and the pressure p of ice solve the stationary nonlinear Stokes problem in Ω:

$$-2\mathrm{div}(\mu\varepsilon(\mathbf{u}))+\nabla p=\rho\mathbf{g}, \tag{1}$$

$$\mathrm{div}(\mathbf{u}) \;=0, \tag{2}$$

where $\varepsilon(\mathbf{u})=\frac{1}{2}(\nabla\mathbf{u}+\nabla\mathbf{u}^T)$ is the rate of strain tensor, μ the viscosity of ice, ρ is the density of ice and $\mathbf{g}$ the gravity force. The viscosity μ of Glen's flow law is a function of $|\varepsilon(\mathbf{u})|:=\sqrt{\varepsilon(\mathbf{u}):\varepsilon(\mathbf{u})}$ with $\varepsilon(\mathbf{u}):\varepsilon(\mathbf{u})=\sum_{i,j=1}^{3}\varepsilon(\mathbf{u})_{ij}^2$, that is uniquely defined by the following nonlinear equation:

$$\frac{1}{2\mu}=A(\tau_0^{n-1}+(\sqrt{2}\mu|\varepsilon(\mathbf{u})|)^{n-1}), \tag{3}$$

where A is a positive parameter, $n\geq 1$ is Glen's exponent and $\tau_0>0$ is a small regularization parameter. When $n=1$, then μ is constant and equations (1) (2) correspond to the classical linear Stokes problem related to a Newtonian fluid [4, 8]. In the framework of glaciology, n is often taken equal to 3, see [13]. Equations (1) (2) are supplied by three kind of conditions on the boundary of Ω. First, no force applies on the ice-air interface, then we have the following Neumann condition:

$$2\mu\varepsilon(\mathbf{u})\cdot\mathbf{n}-p\mathbf{n}=\mathbf{0}, \qquad \text{on } \Gamma_N, \tag{4}$$

where $\mathbf{n}$ is the unit outward normal vector along the boundary of the domain Ω. Second, a zero-Dirichlet condition applies on the no-sliding ice-bedrock interface, then we have the following Dirichlet condition:

$$\mathbf{u}=\mathbf{0}, \qquad \text{on } \Gamma_D. \tag{5}$$

Third, a nonlinear sliding condition [12, 14, 20] applies on the remaining ice-bedrock interface, then we have the following Dirichlet-Robin condition:

$$\mathbf{u}\cdot\mathbf{n}=0, \qquad (2\mu\varepsilon(\mathbf{u})\cdot\mathbf{n})\cdot\mathbf{t}_i=-\alpha\mathbf{u}\cdot\mathbf{t}_i \quad i=1,2 \quad \text{on } \Gamma_R, \tag{6}$$

where $\{\mathbf{t}_i\}_{i=1,2}$ are two orthogonal vectors tangent to the boundary Γ_R and $\alpha=\alpha(|\mathbf{u}|)$ is the sliding coefficient that is given by:

$$\alpha(|\mathbf{u}|)=c(|\mathbf{u}|+t_0)^{\frac{1}{n}-1}, \tag{7}$$

where n is Glen's exponent, c is a positive parameter and $t_0>0$ is a small regularisation parameter.

1.2 Well-posedness of problem (1) - (7)

To analyse the problem (1) - (7), one needs to introduce the next two Banach spaces for velocity and pressure fields

$$V:=\{\mathbf{v}\in[W^{1,r}(\Omega)]^3, \quad \mathbf{v}=\mathbf{0} \text{ on } \Gamma_D,\ \mathbf{v}\cdot\mathbf{n}=0 \text{ on } \Gamma_R\}, \qquad Q:=L^{r'}(\Omega), \tag{8}$$

where $r := 1 + 1/n$ and $r' := n + 1$ are conjugate exponents related to Glen's exponent n. The weak form of problem (1) - (7) with boundary conditions (4) (5) (6) consists of finding $(\mathbf{u}, p) \in V \times Q$ such that

$$2\int_\Omega \mu(|\varepsilon(\mathbf{u})|)\varepsilon(\mathbf{u}) : \varepsilon(\mathbf{v})dV + \sum_{i=1,2}\int_{\Gamma_R} \alpha(|\mathbf{u}|)(\mathbf{u}\cdot\mathbf{t}_i)(\mathbf{v}\cdot\mathbf{t}_i)dS \tag{9}$$

$$-\int_\Omega p\,\mathrm{div}(\mathbf{v})dV + \int_\Omega q\,\mathrm{div}(\mathbf{u})dV = \rho\int_\Omega \mathbf{g}\cdot\mathbf{v}dV, \tag{10}$$

for all $(\mathbf{v}, q) \in V \times Q$. We can check (see [13, 17]) that the weak formulation (9) (10) is meaningful by using the definition (7) of α and the behaviour of μ as function of $s = |\varepsilon(\mathbf{u})|$ which satisfies:

$$\frac{C_1}{(1+s)^{1-\frac{1}{n}}} \le \mu(s) \le \frac{C_2}{(1+s)^{1-\frac{1}{n}}}, \quad \forall s \ge 0, \tag{11}$$

where C_1, C_2 are positive constants. To eliminate the pressure field in the formulation (9) (10), we consider the divergence-free velocity space:

$$V_{div} := \{\mathbf{v} \in V, \quad \mathrm{div}(\mathbf{v}) = 0, \quad \mathbf{v} = \mathbf{0} \text{ on } \Gamma_D, \quad \mathbf{v}\cdot\mathbf{n} = 0 \text{ on } \Gamma_R\}. \tag{12}$$

Then, the reduced formulation consists of finding $\mathbf{u} \in V_{div}$ such that:

$$2\int_\Omega \mu(|\varepsilon(\mathbf{u})|)\varepsilon(\mathbf{u}) : \varepsilon(\mathbf{v})dV + \sum_{i=1,2}\int_{\Gamma_R} \alpha(|\mathbf{u}|)(\mathbf{u}\cdot\mathbf{t}_i)(\mathbf{v}\cdot\mathbf{t}_i)dS = \rho\int_\Omega \mathbf{g}\cdot\mathbf{v}dV, \tag{13}$$

for all $\mathbf{v} \in V_{div}$. Problem (13) rewrites as a minimization problem in V_{div} for the functional:

$$J(\mathbf{u}) := \int_\Omega \left(\int_0^{|\varepsilon(\mathbf{u})|} s\mu(s)ds\right)dV + \frac{1}{2}\int_{\Gamma_R}\left(\int_0^{|\mathbf{u}|} t\alpha(t)dt\right)dS - \rho\int_\Omega \mathbf{u}\cdot\mathbf{g}dV. \tag{14}$$

Using (3), (7) and Korn's inequality, one can prove the strong continuity of J in V, the strict convexity of J, and the coercivity property:

$$J(\mathbf{v}) \ge D_1\|\mathbf{v}\|^r_{W^{1,r}} - D_2, \tag{15}$$

for all $\mathbf{v} \in V$, and for constants $D_1, D_2 > 0$. Continuity, strict convexity and coercivity of J are proved in lemma 3.5, lemma 3.6 and lemma 3.7 in [17], respectively. The existence and the uniqueness of a minimizer (and then of a solution of the reduced problem (13)) follows from arguments of convex analysis, see the details in [13, 17]. Moreover, we can show that the spaces V and Q satisfy the inf-sup condition [13, 17]:

$$C < \inf_{q\in Q}\sup_{\mathbf{v}\in V} \frac{\int_\Omega q\,\mathrm{div}(\mathbf{v})dV}{\|q\|_{L^{r'}}\|\mathbf{v}\|_{W^{1,r}}}, \tag{16}$$

for a constant $C > 0$. This inf-sup condition ensures the existence of a unique of $p \in Q$ such that $(\mathbf{u}, p)$ satisfies the mixed formulation (9) (10), see [4]. Finally, we have the next theorem.

Theorem 1 ([17]). *There exists a unique couple $(\mathbf{u}, p) \in (V, Q)$ satisfying the weak formulation (9) (10).*

1.3 Numerical approximation of problem (1) - (7)

In this subsection, we assume that Ω is a convex polyhedral domain and $\mathscr{T}_H$ is a regular tetrahedral mesh of $\overline{\Omega}$ parametrised by H, the highest diameter of the elements of $\mathscr{T}_H$. Call $V_H \subset V$ and $Q_H \subset Q$ some finite dimensional approximation spaces on $\mathscr{T}_H$ of V and Q that satisfy the inf-sup condition (16) when replacing V and Q by V_H and Q_H. The discrete problem consists of finding $(\mathbf{u}_H, p_H) \in (V_H, Q_H)$ such that:

$$2\int_\Omega \mu(|\varepsilon(\mathbf{u}_H)|)\varepsilon(\mathbf{u}_H) : \varepsilon(\mathbf{v}_H)dV + \sum_{i=1,2}\int_{\Gamma_R} \alpha(|\mathbf{u}_H|)(\mathbf{u}_H \cdot \mathbf{t}_i)(\mathbf{v}_H \cdot \mathbf{t}_i)dS \quad (17)$$

$$-\int_\Omega p_H \,\mathrm{div}\mathbf{v}_H dV + \int_\Omega q_H \,\mathrm{div}\mathbf{u}_H dV = \rho\int_\Omega \mathbf{g}\cdot\mathbf{v}_H dV, \quad (18)$$

for all $(\mathbf{v}_H, q_H) \in (V_H, Q_H)$. The existence and the uniqueness of a solution of the discrete problem (17) (18) can be proved by using the same arguments than for problem (9) (10), when replacing V and Q by V_H and Q_H.

The error between the solution of the exact problem (9) (10) and the solution of the discrete problem (17) (18) can be analysed by following the arguments of [1, 3, 9]. First, the method consists of analysing the error using a quasi-norm that depends on the solution $\mathbf{u}$, see [1]. Second, we deduce an inequality in standard norms (theorem 3.8 in [17]) by using some properties of the quasi-norm. Eventually, interpolation inequalities yield to an *a priori* estimate in the next theorem.

Theorem 2 ([17]). *Assume that, for all $\kappa \in [r, 2]$, there exists a continuous operator $\pi_H : [W^{2,\kappa}]^3 \longrightarrow V_H$ that satisfies:*

$$\|\mathbf{v} - \pi_H(\mathbf{v})\|_{W^{1,\kappa}} \leq Ch\|\mathbf{v}\|_{W^{2,\kappa}}, \qquad \forall \mathbf{v} \in [W^{2,\kappa}]^3, \quad (19)$$

and a continuous operator $\rho_H : W^{1,\kappa'} \longrightarrow Q_H$ that satisfies:

$$\|q - \rho_H(q)\|_{L^{\kappa'}} \leq Ch\|q\|_{W^{1,\kappa'}}, \qquad \forall q \in W^{1,\kappa'}, \quad (20)$$

where κ' is such that $1/\kappa + 1/\kappa' = 1$. Assume V_H and Q_H satisfy the inf-sup condition (16). Let $(\mathbf{u}, p)$ be the solution of problem (9) (10) and let $(\mathbf{u}_H, p_H)$ be the solution of problem (17) (18). If $(\mathbf{u}, p) \in ([W^{2,\kappa}]^3, W^{1,\kappa'})$, where $\kappa \in [r, 2]$, then we have:

$$\|\mathbf{u} - \mathbf{u}_H\|_{W^{1,r}} + \left(\|p - p_H\|_{L^{\kappa'}}\right)^{\frac{\kappa'}{2}} \leq D\, h^{\frac{\kappa}{2}}, \quad (21)$$

where $D = D(\|\mathbf{u}\|_{W^{2,\kappa}}, \|p\|_{W^{1,\rho}}) > 0$.

The estimate (21) suggests a linear convergence with respect to H as long as the solution is sufficiently smooth, i.e. $(\mathbf{u}, p) \in ([W^{2,2}]^3, W^{1,2})$. However, numerical experiences [17] have shown intact order of convergence with less regular solutions. This suggests the non-optimality of the estimate (21), as noticed in [9] for a comparable problem.

2 Evolution problem

2.1 Model

In this section, we consider the time dependent problem that couples the Stokes equation of Section 1 to a transport equation. Let t be the time variable that ranges in the interval $[0,T]$. At each time t, the velocity field $\mathbf{u}(t)$ solves the stationary Stokes problem (1) - (7) in the domain of ice $\Omega(t)$, with boundaries $\Gamma_D(t)$, $\Gamma_N(t)$ and $\Gamma_R(t)$. Since glaciers take complex shapes with changing topologies, we opt for an Eulerian formulation to describe the changes of the ice geometry $\Omega(t)$ [19].

Call Λ a cavity of $\mathbb{R}^3$ that contains $\Omega(t)$ at any time $t \in [0,T]$. The presence of ice in Λ is described by the characteristic function (called later volume fraction of ice) [16, 19] $\varphi : \Lambda \times (0,T) \to \mathbb{R}$ defined by:

$$\varphi(x,y,z,t) = \begin{cases} 1, & \text{if } (x,y,z) \in \Omega(t), \\ 0, & \text{else.} \end{cases} \tag{22}$$

The mass conservation principle [14, 16] leads to the following transport equation for the volume fraction of ice :

$$\frac{\partial \varphi}{\partial t} + \mathbf{u} \cdot \nabla \varphi = b \delta_{\Gamma_N(t)}, \tag{23}$$

where $b(x,y,z,t)$ is the height of ice added or removed due to precipitation and melting and $\delta_{\Gamma_N(t)}$ is the density of surface (or Dirac measure) on the ice-air interface $\Gamma_N(t)$. Since φ is discontinuous across the interface ice-air, equation (23) must be understood in a weak sense.

2.2 Numerical approximation

Let $0 = t^0 < t^1 < ... < t^N = T$ be a uniform subdivision of the time interval $[0,T]$. Call $\mathbf{u}^n$ and φ^n some approximations of $\mathbf{u}$ and φ at time n. At each time step n, problems (1) - (7) and (23) are solved successively. First, we find $\mathbf{u}^n$ by solving the diffusion problem (1) - (7) on Ω^n, the ice domain being defined by the volume

fraction of ice φ^n. Second, we find φ^{n+1} by solving the advection problem (23) from φ^n and $\mathbf{u}^n$.

Diffusion and advection problems are advantageously solved on two different fixed meshes, denoted $\mathscr{T}_H$ and $\mathscr{T}_h$, respectively, see [2, 16, 18] and Fig. 2. Indeed, on one hand, the complex shape of bedrock topographies incites us to use an unstructured mesh ($\mathscr{T}_H$, where H is the typical size of a tetrahedron). On a second hand, the advection problem (23) is easier to solve on a structured grid made of cells ($\mathscr{T}_h$, where h is the size of cells). Moreover, $\mathscr{T}_h$ can be chosen finer since the advection problem (23) is less CPU time consuming than the diffusion problem. The fine mesh allows us to reduce the numerical diffusion of the free surface Γ_N. A good trade-off between accuracy and efficiency is $H \simeq 5h$, see [18]. Note that $\mathscr{T}_H$ fits the bedrock from below but is built higher than the surface of ice at any time while $\mathscr{T}_h$ covers the whole cavity Λ, see Fig. 2. Transfer of variables φ^n and $\mathbf{u}^n$ between meshes $\mathscr{T}_h$ and $\mathscr{T}_H$ are ensured by linear interpolations.

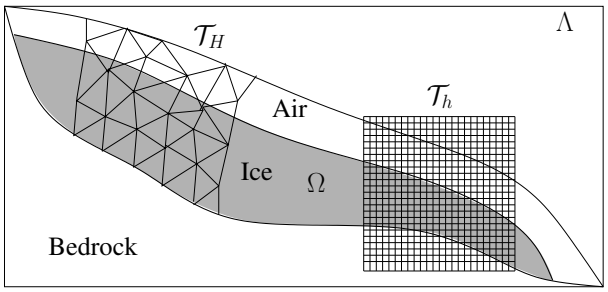

Fig. 2 Exemple of the space discretisation: $\mathscr{T}_H$ is an unstructured mesh that fits the bedrock topography while $\mathscr{T}_h$ is a finer grid overlapping $\mathscr{T}_H$.

On one part of the mesh $\mathscr{T}_H$, we implement a finite element method to solve the diffusion problem (1) - (7). First, we select the elements of $\mathscr{T}_H$ that are on the ice domain by using the nodal values of φ^n on $\mathscr{T}_H$ [18]. Second, we use continuous, piecewise linear finite elements for the velocity and pressure fields to solve (1) - (7). Since this choice of space is not stable for satisfying the inf-sup condition (16), see Subsection 1.3, one can either enrich the space of velocities by a bubble function or add a stabilisation term in the discrete variational formulation [6, 14]. We opt for the latter. A fixed point method is used to solve the nonlinearity due to the non-linear viscosity (3), see [16].

On the regular grid $\mathscr{T}_h$, we implement the method of characteristics to solve the advection problem (23). For each cell of $\mathscr{T}_h$, the volume fraction of ice φ^n is advected according to the velocity field $\mathbf{u}^n$, and then projected onto the grid $\mathscr{T}_h$, see [16, 18]. An additional algorithm, SLIC (Simple Line Interface Calculation), reduces the numerical diffusion of φ that is introduced during the projection step [19]. To account for the right-hand-side of the equation (23), the volume fraction of ice of surface cells are filled or emptied according to $b(t^n)$, see [16]. The resulting

transport algorithm is unconditionally stable and CFL numbers greater than one can be used.

We refer to [14, 16, 18] for more details about the advection and diffusion steps.

2.3 Simulation of Aletschgletscher

Aletschgletscher, Switzerland, is the largest glacier of the European Alps. In 1999, it had a length of about 22 km, an area of about 83 km^2 and a volume of ice of about 15 km^3 [5]. The numerical simulation of this glacier from 1880 to 1999 was performed in [13, 15] and proved to reproduce accurately the observations after fitting parameters A and c.

This experiment aims to simulate Aletschgletscher over the 21st century according to a plausible climatic scenario. To be as realistic as possible, we opt for the median scenario of the regional climate models given in [7] which predicts an increase of the temperature of 3.8°C during the 21st century. From this climatic trend, we simulate the daily snow precipitations and the melting everywhere on the glacier from 1999 to 2100 [11, 15]. Summing the ice accumulation and ablation over each year gives the mass balance function b to be used in (23).

The bedrock topography of Aletschgletscher was reconstructed from measurements [5], and the elevation of the ice surface is available for 1999. From these data, the two meshes $\mathscr{T}_H$ and $\mathscr{T}_h$ are generated as described in [14]. The size of the meshes is: $H \sim 100$ m and $h = 20$ m. The time step 0.5 year proves to be a good trade-off between efficiency and stability. Physical parameters are chosen as follows. Glen's exponent n is set to 3 and the regularisation parameters are set to $\tau_0 = \sqrt{0.1}$ bar and $t_0 = 0 = 0.01$ m a^{-1}. Sliding effects are only accounted below the altitude 2400 m a.s.l [15] (Γ_R), while above ice is supposed to be fixed to the bedrock (Γ_D). The rate factor A and the sliding coefficient c are calibrated such that they minimize the mean-square error between computed and measured ice surface velocities, see [15]. As a result, we obtain $A = 0.1$ bar^{-3} a^{-1} and $c = 0.3$ bar $\text{m}^{-1/3}$ $\text{a}^{1/3}$.

Snapshots each 25 years of the simulation are displayed in Fig. 3. According to our simulation, Aletschgletscher will continue to decay until almost disappearing by 2100 if the climate should indeed follow the trend of the chosen scenario. Note that, if the retreat remains limited until 2050, one should expect a strong acceleration of the retreat rate after 2050.

Acknowledgements The first author was supported by the Deutsche Forschungsgemeinschaft (project KL 1806 5-1).

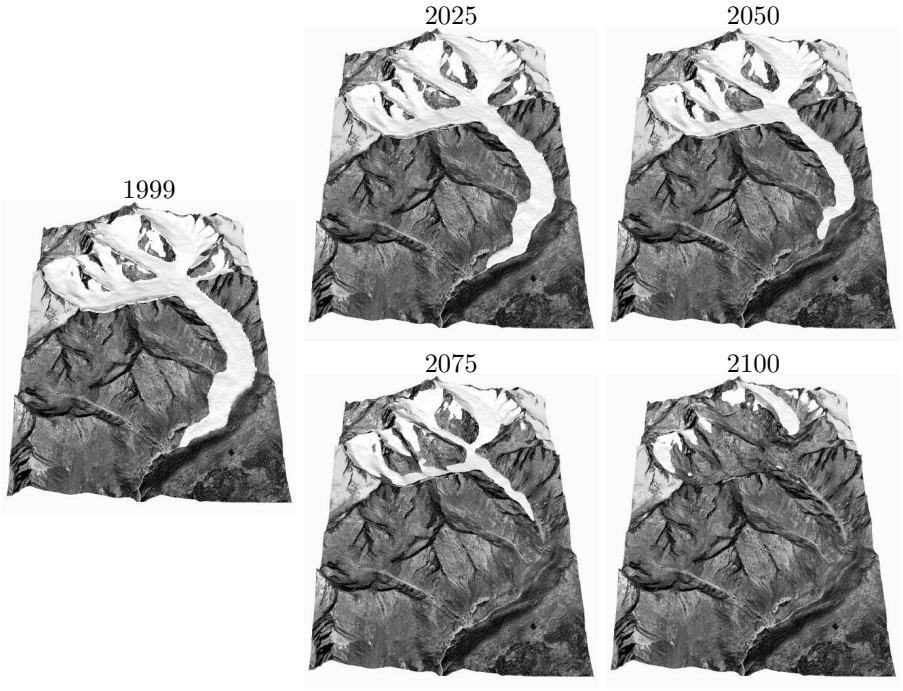

Fig. 3 Aletschgletscher in 1999 (initialisation), 2025, 2050, 2075 and 2100 according to the simulation.

References

1. J. W. Barrett and W. B. Liu. Quasi-norm error bounds for the finite element approximation of a non-Newtonian flow. *Numer. Math.*, 68(4):437–456, 1994.
2. A. Caboussat, G. Jouvet, M. Picasso, and J. Rappaz. Numerical algorithms for free surface flow. *Book chapter in CRC volume 'Computational Fluid Dynamics'*, 2011.
3. J. Colinge and J. Rappaz. A strongly nonlinear problem arising in glaciology. *M2AN Math. Model. Numer. Anal.*, 33(2):395–406, 1999.
4. A. Ern and J.L. Guermond. *Theory and practice of finite elements*. Springer, 2004.
5. D. Farinotti, M. Huss, A. Bauder, M. Funk, and M. Truffer. A method to estimate ice volume and ice thickness distribution of alpine glaciers. *J. Glaciol.*, 55(191):422–430, 2009.
6. L. P. Franca and S. L. Frey. Stabilized finite element methods. II. The incompressible Navier-Stokes equations. *Comput. Methods Appl. Mech. Engrg.*, 99(2-3):209–233, 1992.
7. C. Frei. Die Klimazukunft der Schweiz. In *Klimaänderung und die Schweiz 2050 – Erwartete Auswirkungen auf Umwelt, Gesellschaft und Wirtschaft*, pages 12–16. Beratendes Organ für Fragen der Klimaänderung (OcCC), 2007. http://www.occc.ch.
8. V. Girault and P.A. Raviart. *Finite Element Methods for Navier-Stokes Equations: Theory and Algorithms*. Springer Series in Computational Mathematics, 1986.
9. R. Glowinski and J. Rappaz. Approximation of a nonlinear elliptic problem arising in a non-Newtonian fluid flow model in glaciology. *M2AN Math. Model. Numer. Anal.*, 37(1):175–186, 2003.
10. R. Greve and H. Blatter. *Dynamics of Ice Sheets and Glaciers*. Springer Verlag, 2009.
11. M. Huss, A. Bauder, M. Funk, and R. Hock. Determination of the seasonal mass balance of four alpine glaciers since 1865. *Journal of Geophysical Research*, 113, 2008.

12. K. Hutter. *Theoretical Glaciology*. Reidel, 1983.
13. G. Jouvet. *Modélisation, analyse mathématique et simulation numérique de la dynamique des glaciers*. PhD thesis, EPF Lausanne, 2010.
14. G. Jouvet, M. Huss, H. Blatter, M. Picasso, and J. Rappaz. Numerical simulation of rhonegletscher from 1874 to 2100. *J. Comp. Phys.*, 228:6426–6439, 2009.
15. G. Jouvet, M. Huss, M. Funk, and H. Blatter. Modelling the retreat of Grosser Aletschgletscher, Switzerland, in changing climate. *J. Glaciol.*, 57(206):1033–1045, 2011.
16. G. Jouvet, M. Picasso, J. Rappaz, and H. Blatter. A new algorithm to simulate the dynamics of a glacier: theory and applications. *J. Glaciol.*, 54(188):801–811, 2008.
17. G. Jouvet and J. Rappaz. Analysis and finite element approximation of a nonlinear stationary stokes problem arising in glaciology. *Advances in Numerical Analysis, Hindawi Publishing Corp., Article ID 164581*, 2011, 2011.
18. V. Maronnier, M. Picasso, and J. Rappaz. Numerical simulation of three-dimensional free surface flows. *Internat. J. Numer. Methods Fluids*, 42(7):697–716, 2003.
19. R. Scardovelli and S. Zaleski. Direct numerical simulation of free-surface and interfacial flow. *Ann. Rev. Fluid Mech.*, 31(7):567–603, 1999.
20. C. Schoof. Coulomb friction and other sliding laws in a higher order glacier flow model. *Mathematical Models and Methods in Applied Sciences*, 2009.